

LEAD THE RACE

Comprehensive **flow cytometry** solutions designed to accelerate your work



Learn More

MILLIPORE
SIGMA



The Journal of
Immunology

In This Issue

J Immunol 2018; 200:1231-1232; ;

doi: 10.4049/jimmunol.1790027

<http://www.jimmunol.org/content/200/4/1231>

This information is current as
of February 7, 2018.

Why *The JI*?

- **Rapid Reviews! 30 days*** from submission to initial decision
- **No Triage!** Every submission reviewed by practicing scientists
- **Speedy Publication!** 4 weeks from acceptance to publication

**average*

Subscription Information about subscribing to *The Journal of Immunology* is online at:
<http://jimmunol.org/subscription>

Permissions Submit copyright permission requests at:
<http://www.aai.org/About/Publications/JI/copyright.html>

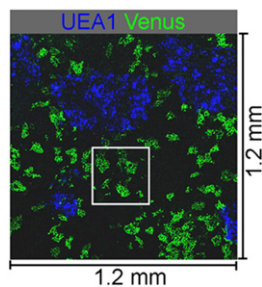
Email Alerts Receive free email-alerts when new articles cite this article. Sign up at:
<http://jimmunol.org/alerts>

The Journal of Immunology is published twice each month by
The American Association of Immunologists, Inc.,
1451 Rockville Pike, Suite 650, Rockville, MD 20852
Copyright © 2018 by The American Association of
Immunologists, Inc. All rights reserved.
Print ISSN: 0022-1767 Online ISSN: 1550-6606.



Quantifying Previously Lost Epithelial Cells

Cortical thymic epithelial cells (cTECs) and medullary (m)TECs support the structure and function of the thymus. The majority of cTECs specifically express the proteasome component $\beta 5t$, whereas mTECs express the nuclear protein Aire. Adult mouse thymic tissue has been estimated to contain 10^4 cTECs and 10^5 mTECs. However, these estimates have relied on conventional isolation procedures requiring enzymatic digestion, a protocol that may result in cellular depletion. To determine whether cTEC and mTEC numbers have been systematically underestimated, Sakata et al. (p. 1382) used a manual counting and three-dimensional summing approach to calculate the number of TECs in thymic lobes of 5–6 wk old C57BL/6 mice. Thymic sections were stained for CD4 and CD8 to visualize thymocytes and for mTEC-reactive anti-keratin 5 Ab to distinguish the cortical and medullary microenvironments. Parallel experiments demonstrated that thymocyte cellularity calculated via flow cytometry was approximately half (60% for $CD4^+CD8^+$ thymocytes and 40% for $CD4^+CD8^-$ thymocytes) of that measured by section analysis, suggesting that preparation methods for flow cytometric analysis deplete thymocytes. Next, thymic sections were stained to distinguish cTECs and mTECs. Aire⁺ mTECs were quantified at $4.9 \times 10^5 \pm 5.8 \times 10^4$ cells in the right thymic lobe; $\beta 5t^+$ cTECs totaled $3.7 \times 10^5 \pm 4.2 \times 10^4$ cells per right thymic lobe. These data demonstrate that thymi of postnatal mice contain $\sim 9 \times 10^5$ $\beta 5t^+$ cTECs and 1.1×10^6 Aire⁺ mTECs, numbers 10 to nearly 100-fold larger than previously estimated using conventional enzymatic digestion.



Caspase-8 Loss in DCs Enhances Antiviral Responses

Caspase-8 (CASP8) is a mediator of death receptor-mediated apoptosis and a negative regulator of necroptosis and retinoic acid-inducible gene I (RIG-I) signaling. However, in dendritic cells (DCs), loss of CASP8 does not enhance necroptosis. To examine the effects of CASP8 loss in DCs, Tsau et al. (p. 1335) generated conditional knockout mice lacking DC-specific *Casp8* (*dcCasp8*^{-/-}). Compared with control (*Casp8*^{fllox/fllox}) mice, *dcCasp8*^{-/-} mice displayed increased proportions of hyperactive conventional DCs (cDCs) and $CD4^+$ T cells at 3 mo of age and activated $CD8^+$ T cells at 6 mo of age. In 10-mo-old *dcCasp8*^{-/-} mice, splenic architecture was disrupted, with

increased white pulp, and livers contained increased polymorphic infiltrates, suggestive of an autoimmune phenotype. Surprisingly, splenic regulatory T cells were increased in both percentage and number in *dcCasp8*^{-/-} mice. Given their enhanced development of activated cDCs and T cells, the authors investigated the ability of *dcCasp8*^{-/-} mice to mount an immune response to chronic infection with lymphocytic choriomeningitis virus (LCMV). LCMV-specific $CD4^+$ T cells expanded and were less exhausted in infected *dcCasp8*^{-/-} compared with control mice. Moreover, a higher proportion of both $CD4^+$ and $CD8^+$ T cells were polyfunctional and viral load was reduced in *dcCasp8*^{-/-} mice. To determine whether cDC hyperactivation was cell-extrinsic, *Casp8*^{-/-} $CD11c^+$ cells were transfected with polyinosinic-polycytidylic acid [poly(I:C)], which activates RIG-I. The poly(I:C)-transfected *Casp8*^{-/-} cDCs upregulated CD86 to a greater degree and secreted more IFN- γ , TNF- α , IL-6, and MCP-1 into culture supernatants, compared with identically treated cDCs from control mice. *Casp8*^{-/-} bone marrow-derived DCs and activated *Casp8*^{-/-} splenic cDCs transfected with poly(I:C) showed enhanced expression of phosphorylated IFN regulatory factor 3, which is cleaved by CASP8. Taken together, these data underscore the importance of DC hypersensitivity in modulating T cell responses and reveal that *dcCasp8*^{-/-} mice develop symptoms of autoimmune disease and mount an enhanced immune response to LCMV.

Interplay of IL-13 and IL-33 in Obesity

Helper 2 cytokines, including IL-13, are known to regulate glucose tolerance and overcome insulin resistance in obesity. However, the role of the IL-13 decoy receptor IL-13R $\alpha 2$ (which lowers IL-13 bioactivity) in regulation of metabolic homeostasis is not well understood.

IL-33 induces protective effects in adipose tissue inflammation, but the interplay between IL-13 and IL-33 in obesity remains unclear. Thus, Duffen et al. (p. 1347) examined the modulation of the IL-33/IL-13 axis in obesity. Mice fed a high fat diet (HFD) had increased IL-13R $\alpha 2$ mRNA in adipose tissue and soluble IL-13R $\alpha 2$ in the serum. Compared with mice on chow diet, wild type (wt) mice fed HFD displayed elevated IL-13R $\alpha 2$ in epididymal white adipose tissue (eWAT), which is associated with insulin resistance, but not in s.c. fat (scWAT), which is associated with enhanced insulin action. The authors found that HFD alone was not sufficient to affect systemic metabolic responses in *il13ra2*^{-/-} mice and thus used exogenous IL-33 to induce IL-13. IL-13 was significantly increased in eWAT and scWAT of IL-33-treated *il13ra2*^{-/-} mice compared with wt mice on chow diet. IL-33 administration



induced expression of genes encoding Th2 cytokines IL-13, IL-4, and IL-5 in eWAT of wt mice fed HFD, whereas the expression of these genes was reduced in eWAT of *il13 α 2*^{-/-} mice. In contrast, the expression of IL-5 was elevated in eWAT of *il13*^{-/-} mice, suggesting that IL-13 negatively regulates IL-5. Eosinophilic inflammation was increased in *il13*^{-/-} mice. Moreover, *il13*^{-/-} mice were protected from gastrointestinal effects seen in wt mice in response to IL-33 administration. Overall, IL-33 administration facilitates weight loss on HFD and reduces insulin and fasting glucose levels. Taken together, the data demonstrate that IL-13R α 2 deficiency ameliorates the metabolic consequences of HFD, in the context of IL-33 administration, and reveal a regulatory role for IL-13 in limiting tissue inflammation in response to IL-33.

Autoreactive T Cells Mediate Allograft Rejection

T cell-mediated rejection is the primary obstacle to achieving tolerance in type 1 diabetes patients who receive whole pancreas or pancreatic islet transplants. Whereas studies have suggested that active autoimmunity directed toward islets contributes to the rejection of pancreatic or islet allografts, it is unknown how recognition by autoreactive T cells of self-peptides presented within self-MHC molecules contributes to rejection of MHC-mismatched transplanted tissues. In this issue, Burrack et al. (p. 1504) demonstrated

that ~17% of autoreactive CD4⁺ T cells expressing islet-reactive self-MHC-restricted TCRs derived from NOD mice spontaneously reacted against allogeneic spleen cells in vitro. At the time of rejection, total RNA from the endogenous pancreatic islets and transplanted grafts was isolated and analyzed by high-throughput sequencing to identify TCRs associated with autoimmune diabetes (TCRs expressed by pancreas-derived T cells) or graft rejection (TCRs expressed by T cells detected in the transplanted tissues). TCRs expressed by pancreas-derived T cells were also found in MHC-mismatched (C3H) islet transplants in NOD mice. Furthermore, pancreas-derived TCRs accumulated at a higher frequency in grafts than TCRs detected solely in the allograft, suggesting a rapid accumulation of autoreactive T cells in allogeneic grafts. Analysis of the most prevalent TCR sequences in C3H allografts with robust infiltration of autoreactive NOD pancreas-derived T cells revealed six NOD pancreas-derived sequences that also displayed allogeneic responsiveness against irradiated CH3 spleen cells in vitro. Of these six TCRs displaying dual allo- and autoreactive activity, all recognized donor C3H MHC molecules. Finally, five of the six dual-reactive TCRs responded to NOD insulinoma β cell-derived NIT-1 cells, confirming the alloreactive response to syngeneic islet cells. Collectively, these data demonstrate that autoreactive T cells can mediate heterologous alloreactivity, and suggest that successful transplantation of allogeneic tissue into individuals with autoimmunity may require suppression of autoreactive memory/effector T cells.